**Ahmed K. Noor**
**Jeanne M. Peters**
*Center for Computational Structures Technology*
*University of Virginia*
*NASA Langley Research Center*
*Hampton, VA 23681*

# Nonlinear Vibrations of Thin-Walled Composite Frames

*A reduced basis technique and a computational procedure are presented for generating the nonlinear vibrational response, and evaluating the first-order sensitivity coefficients of thin-walled composite frames. The sensitivity coefficients are the derivatives of the nonlinear frequency with respect to the material and lamination parameters of the frame. A mixed formulation is used with the fundamental unknowns consisting of both the generalized displacements and stress resultants in the frame. The flanges and webs of the frames are modeled by using geometrically nonlinear two-dimensional shell and plate finite elements. The computational procedure can be conveniently divided into three distinct steps. The first step involves the generation of various-order perturbation vectors, and their derivatives with respect to the material and lamination parameters of the frame, using the Linstedt–Poincaré perturbation technique. The second step consists of using the perturbation vectors as basis vectors, computing the amplitudes of these vectors and the nonlinear frequency of vibration, via a direct variational procedure. The third step consists of using the perturbation vectors, and their derivatives, as basis vectors and computing the sensitivity coefficients of the nonlinear frequency via a second application of the direct variational procedure. Numerical results are presented for semicircular thin-walled frames with I and J sections, showing the convergence of the nonlinear frequency and the sensitivity coefficients obtained by both the reduced-basis and perturbation techniques.* © *1994 John Wiley & Sons, Inc.**

## INTRODUCTION

Significant advances have been made in the development of effective analytical and numerical techniques for the nonlinear vibration analysis of structures. Reviews of some of the techniques developed for beam and plate structures are contained in survey papers (Bert, 1982; Sathyamoorthy, 1982a and b, 1987; Kapania and Yang, 1987; Chia, 1988; Kapania and Raciti, 1989) and two monographs by Nayfeh and Mook (1979) and Chia (1980). However, to our knowledge, none of the reported studies considered the nonlinear vibrations of thin-walled composite frames. Moreover, except for a recent study (Noor et al., 1993), no studies have been reported on the sensitivity of the nonlinear vibrational response to variations in the material and geometric parameters of the structure.

The present study is an attempt to fill this void. Specifically, the objective is to summarize the results of a recent study on the nonlinear vibrational response of thin-walled composite frames and the effects of variations in the material parameters of the individual layers on the nonlinear frequencies of vibration. The frames


Received March 23, 1994; Accepted April 26, 1994.

Shock and Vibration, Vol. 1, No. 5, pp. 415–429 (1994)

CCC 1070-9622/94/050415-15

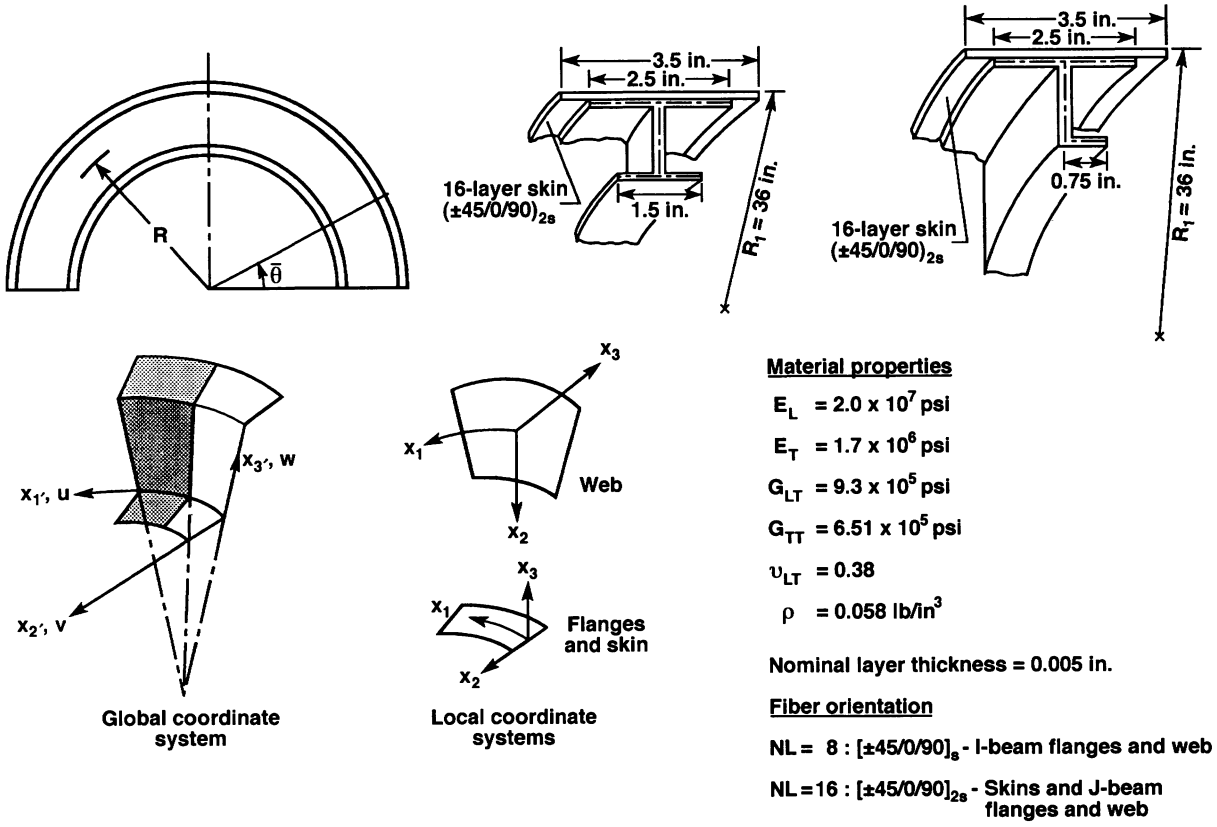


**FIGURE 1** Thin-walled composite frames used in the present study. Subscripts L and T refer to longitudinal (fiber) and transverse directions for each layer, respectively. NL is the total number of layers.

considered are semicircular, made of thin-walled graphite–epoxy material with I and J sections, and have a 36-in. radius (see Fig. 1).

The reduced basis technique was first presented (Noor et al., 1993) and applied to nonlinear vibration analysis of composite plates. The present article adapts the reduced basis technique to the nonlinear vibration analysis of thin-walled composite frames and extends it to the evaluation of the sensitivity coefficients.

The sensitivity information, in addition to being an essential component, is needed for using nonlinear vibration analysis in automated optimum design of composite airframes, and can be used to:

1. generate an approximation for the nonlinear frequency of a modified frame (in conjunction with a reanalysis technique);
2. assess the effects of uncertainties, in the material and geometric parameters of the frame, on the nonlinear frequency; and
3. predict the changes in the nonlinear frequency due to changes in the beam parameters.

## MATHEMATICAL FORMULATION

### Finite Element Model

The spatial discretization is performed by using two-dimensional finite element models based on the moderate-rotation, geometrically nonlinear Sanders–Budiansky type shell theory with the effects of large displacements, transverse shear deformation, laminated anisotropic material response, and rotatory inertia included. A mixed formulation is used in which the fundamental unknowns consist of both the generalized displacements and the stress resultants in the frame.

Bicubic shape functions are used to approximate each of the generalized displacements and stress resultants. There are 16 displacement nodes and 128 stress-resultant parameters in each element. The stress resultants are allowed to be discontinuous at interelement boundaries.

## Variational Equations

For undamped free vibrations of the discretized frame, the variational equations used in evaluating the nonlinear vibrational response and the sensitivity coefficients can be written in the following form:

$$\delta \int_{t_1}^{t_2} (T - \pi) dt = 0 \tag{1}$$

and

$$\delta \int_{t_1}^{t_2} \left( \frac{\partial T}{\partial \lambda} - \frac{\partial \pi}{\partial \lambda} \right) dt = 0 \tag{2}$$

subject to the condition that at times $t = t_1$ and $t = t_2$, the first variations of the fundamental unknowns (generalized nodal displacements and stress-resultant parameters) and their sensitivity coefficients (derivatives with respect to $\lambda$) vanish. In Eqs. (1) and (2), $\lambda$ refers to a typical material, lamination, or geometric parameter of the structure; $T$ and $\pi$ are the kinetic energy and the Hellinger–Reissner functional of the discretized structure given by:

$$T = \frac{1}{2} \left\{ \frac{\partial X}{\partial t} \right\}^T [M] \left\{ \frac{\partial X}{\partial t} \right\} \tag{3}$$

$$\pi = \{H\}^T \left( -\frac{1}{2} [F] \{H\} + [S] \{X\} + \{G(X)\} \right) \tag{4}$$

where $\{H\}$ is the vector of stress-resultant parameters; $\{X\}$ is the vector of nodal displacements; $[M]$ is the consistent mass matrix; $[F]$ is the global flexibility matrix; $[S]$ is the strain-displacement matrix; $\{G(X)\}$ is the vector of nonlinear terms; and superscript $T$ denotes transposition.

The application of the reduced basis technique to the nonlinear vibration and sensitivity analyses of the structure can be conveniently divided into three distinct steps: generating perturbation vectors, and their derivatives with respect to the material, lamination and geometric parameters of the structure, using the Linstedt–Poincaré perturbation technique; using the perturbation vectors as basis (or global approximation) vectors, and computing the amplitudes of these vectors and the nonlinear vibration frequency via a direct variational technique, in conjunction with the method of harmonic balance; and using the perturbation vectors and their derivatives as basis vectors and evaluating the sensitivity coefficients of the nonlinear frequency via a second application of the direct variational technique. The procedure is described subsequently.

## Generation of Perturbation Vectors and Their Derivatives

For the purpose of generating basis vectors, a new independent variable $\tau = \omega t$ is introduced, where $\omega$ is the nonlinear circular frequency. The following expansion is used for $\Omega = \omega^2$, in terms of a small parameter $\varepsilon$:

$$\omega^2 = \Omega(\varepsilon) = \sum_{i=0} \Omega^{(i)} \varepsilon^i. \tag{5}$$

Only the even values of $i$ ($i = 0, 2, 4, \ldots$) are retained in the expansion. The vectors $\{H\}$ and $\{X\}$ are also expanded in perturbation series of the form:

$$\begin{Bmatrix} H(t, \varepsilon) \\ X(t, \varepsilon) \end{Bmatrix} = \sum_{i=1} \begin{Bmatrix} H(\tau) \\ X(\tau) \end{Bmatrix}^{(i)} \varepsilon^i. \tag{6}$$

Each of the time-dependent vectors, $\{H(\tau)\}^{(i)}$ and $\{X(\tau)\}^{(i)}$, are expanded in a Fourier series in $\tau$, and therefore:

$$\begin{Bmatrix} H(t, \varepsilon) \\ X(t, \varepsilon) \end{Bmatrix} = \sum_{i=1} \left( \sum_{m=0}^{i} \begin{Bmatrix} H \\ X \end{Bmatrix}^{(i,m)} \cos m\omega t \right) \varepsilon^i. \tag{7}$$

The equations used in generating the vectors $\begin{Bmatrix} H \\ X \end{Bmatrix}^{(i,m)}$ are obtained by substituting the expansions for $\{H\}$, $\{X\}$, and $\omega^2$, Eqs. (5) and (7), into Eqs. (3), (4) and (1); converting each term into the first power of cosine functions in $t$; and setting the like terms of $\varepsilon$ and $m$ to 0. This leads to a recursive set of linear equations in $\{H\}^{(i,m)}$ and $\{X\}^{(i,m)}$. The explicit form of these equations is given in Noor et al. (1993). Note that the linear free vibration problem corresponds to $i = m = 1$. For each vibration mode (i.e., a prescribed pair of eigenvalue and eigenvector) a set of vectors $\{H\}^{(i,m)}$ and $\{X\}^{(i,m)}$ can be generated. The multipliers of $\varepsilon^i$, that is, the quantity between parentheses in Eq. (7), will henceforth be referred to as the perturbation vectors.

The derivatives of $\omega^2$, $\{H\}$, and $\{X\}$ with respect to the material, lamination, and geometric parameters of the frame are given by:

$$\frac{\partial \omega^2}{\partial \lambda} = \frac{\partial \Omega}{\partial \lambda} = \sum_{i=0} \frac{\partial \Omega^{(i)}}{\partial \lambda} \varepsilon^i \tag{8}$$

and

$$\frac{\partial}{\partial \lambda} \begin{Bmatrix} H(t, \varepsilon) \\ X(t, \varepsilon) \end{Bmatrix} = \sum_{i=1} \left( \sum_{m=0}^{i} \frac{\partial}{\partial \lambda} \begin{Bmatrix} H \\ X \end{Bmatrix}^{(i,m)} \cos m\omega t \right) \varepsilon^i. \tag{9}$$

The equations used in generating $\{\partial H/\partial \lambda\}^{(i,m)}$, $\{\partial X/\partial \lambda\}^{(i,m)}$ are obtained by either: differentiating the governing recursive equations in $\{H\}^{(i,m)}$, $\{X\}^{(i,m)}$ with respect to $\lambda$; or following the same steps used in generating the governing equations for $\{H\}^{(i,m)}$, $\{X\}^{(i,m)}$, but using the functionals in Eq. (2), instead of the functionals in Eq. (1).

In the present study, computerized symbolic manipulation was used in generating the perturbation vectors and their derivatives with respect to $\lambda$. The nonzero terms are associated with either $(i, m)$ even, or $(i, m)$ odd, and are listed in Table 1. All the nonzero coefficients correspond to even values of $i + m$.

## Computation of Amplitudes of Basis Vectors and Nonlinear Frequency

The perturbation vectors in Eq. (7) are now chosen as basis vectors, and the response vectors are expressed as linear combinations of these vectors as follows:

$$\begin{Bmatrix} H \\ X \end{Bmatrix} = \sum_{i=1}^{r} \left( \sum_{m=0}^{i} \begin{Bmatrix} H \\ X \end{Bmatrix}^{(i,m)} \cos m\omega t \right) \psi_i \tag{10}$$

where $\psi_i$ are unknown parameters representing the amplitudes of the basis vectors; and $r$ is the total number of basis vectors used. Equation (10) is substituted into Eqs. (1), (3), and (4). A direct variational technique is used in conjunction with the method of harmonic balance to approximate Eq. (1) by a system of nonlinear algebraic equations in $\psi_i$ ($i$ = 1 to $r$) and $\omega^2$. The additional equation needed to solve the system is obtained by prescribing either one of the displacement components (linear combination of $\psi_i$) or one of the parameters of $\psi_i$. The additional equation will henceforth be referred to as the constraint condition. The form of the nonlinear algebraic equations in $\psi_i$ and $\omega^2$ is given in Appendix A.

**Table 1. Pairs of $(i, m)$ for Which Perturbation Vectors Are Nonzero**

| $i/m$ | 0 | 1 | 2 | 3 | 4 | 5 | 6 |
|---|---|---|---|---|---|---|---|
| 1 | | 1, 1 | | | | | |
| 2 | 2, 0 | | 2, 2 | | | | |
| 3 | | 3, 1 | | 3, 3 | | | |
| 4 | 4, 0 | | 4, 2 | | 4, 4 | | |
| 5 | | 5, 1 | | 5, 3 | | 5, 5 | |
| 6 | 6, 0 | | 6, 2 | | 6, 4 | | 6, 6 |

## Evaluation of Sensitivity Coefficients of Nonlinear Vibrational Response

The perturbation vectors and their derivatives with respect to $\lambda$ are used in approximating the derivatives of the response vectors as follows:

$$\frac{\partial}{\partial \lambda} \begin{Bmatrix} H \\ X \end{Bmatrix} = \sum_{i=1}^{r} \left( \sum_{m=0}^{i} \frac{\partial}{\partial \lambda} \begin{Bmatrix} H \\ X \end{Bmatrix}^{(i,m)} \cos m\omega t \right) \psi_i + \sum_{i=1}^{r} \left( \sum_{m=0}^{i} \begin{Bmatrix} H \\ X \end{Bmatrix}^{(i,m)} \cos m\omega t \right) \bar{\psi}_i \tag{11}$$

where $\bar{\psi}_i$ are unknown parameters. Equation (11) is used in conjunction with a direct variational technique and the method of harmonic balance to approximate Eq. (2) by a system of linear algebraic equations in $\bar{\psi}_i$ ($i$ = 1 to $r$) and $\partial \omega^2/\partial \lambda$. The additional equation is obtained by differentiating the constraint condition, used in evaluating $\omega^2$, with respect to $\lambda$. The form of the linear algebraic equations in $\partial \psi_i/\partial \lambda$ and $\partial \omega^2/\partial \lambda$ is given in Appendix B.

## NUMERICAL RESULTS

To assess the effectiveness of the proposed reduced basis technique, a number of nonlinear vibration problems of thin-walled composite frames have been solved by this technique. For each problem, the convergence of the sensitivity coefficients obtained by the proposed technique were compared with those obtained by the perturbation technique. Herein, results are presented for semicircular frames with an I-section and a J-section. The dimensions of the frame and the cross sections are given in Fig. 1. The frame sections were made from graphite–epoxy unidirectional tape laid in a manner that resulted in

uniform stiffness properties in the circumferential direction (i.e., the stiffness coefficients are independent of $\bar{\theta}$). The material properties for the individual layers are given in Fig. 1. The laminate stacking sequence was $[\pm 45/0/90]_s$ for the I-section and $[\pm 45/0/90]_{2s}$ for the J-section. Bonded to the outside flange of each frame was a 16-ply $[\pm 45/0/90]_{2s}$, quasiisotropic skin made of the same material. The frame sections were constructed so that the skin would extend 0.5 in. beyond each side of the top flange of the frame. The same frames were studied in Noor et al. (1991), in which the predictions of linear vibration analysis were compared with experiments.

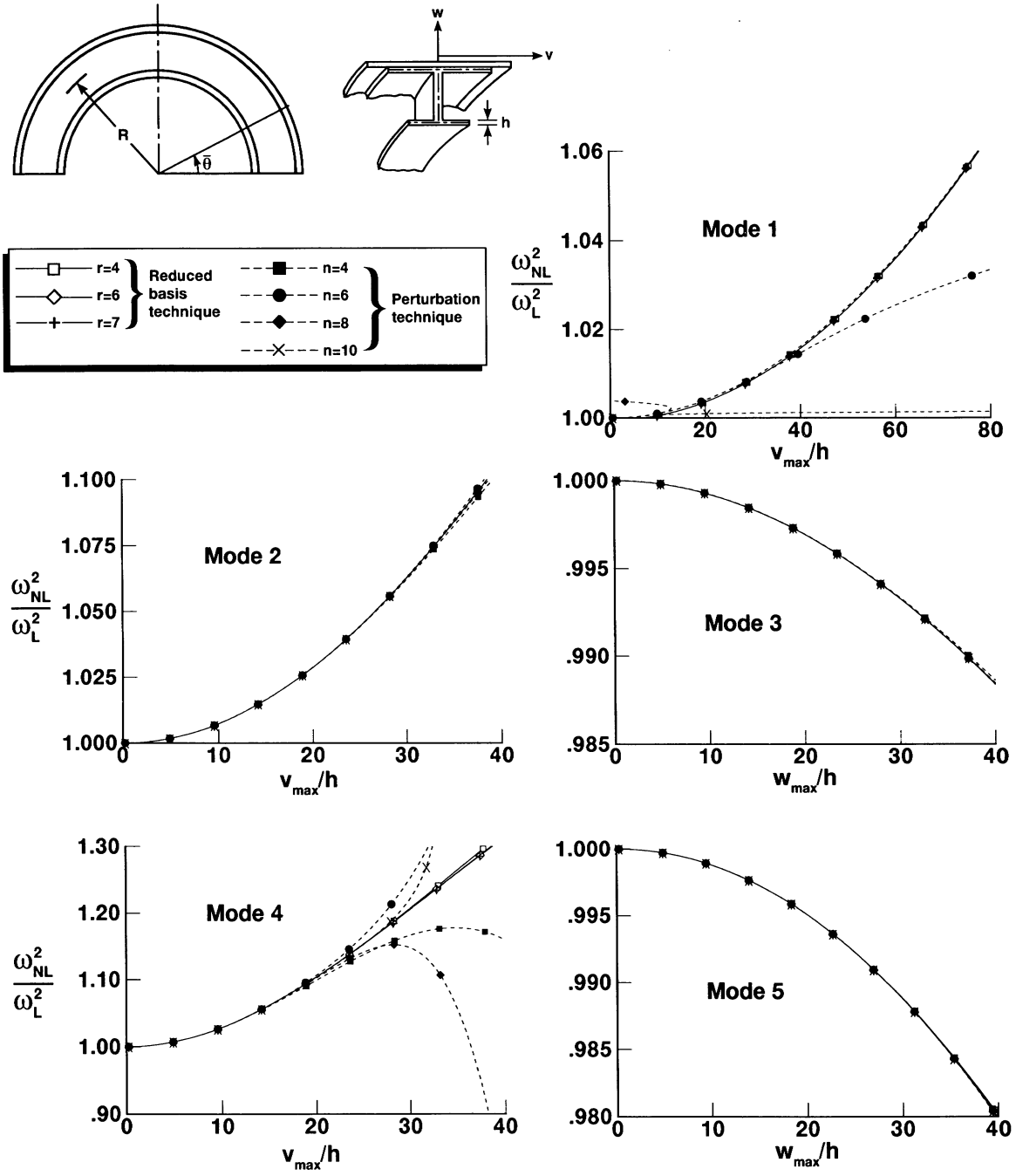


**FIGURE 2** Convergence of nonlinear frequencies obtained by reduced basis and perturbation techniques. Thin-walled composite frame with I cross section (see Fig. 1).

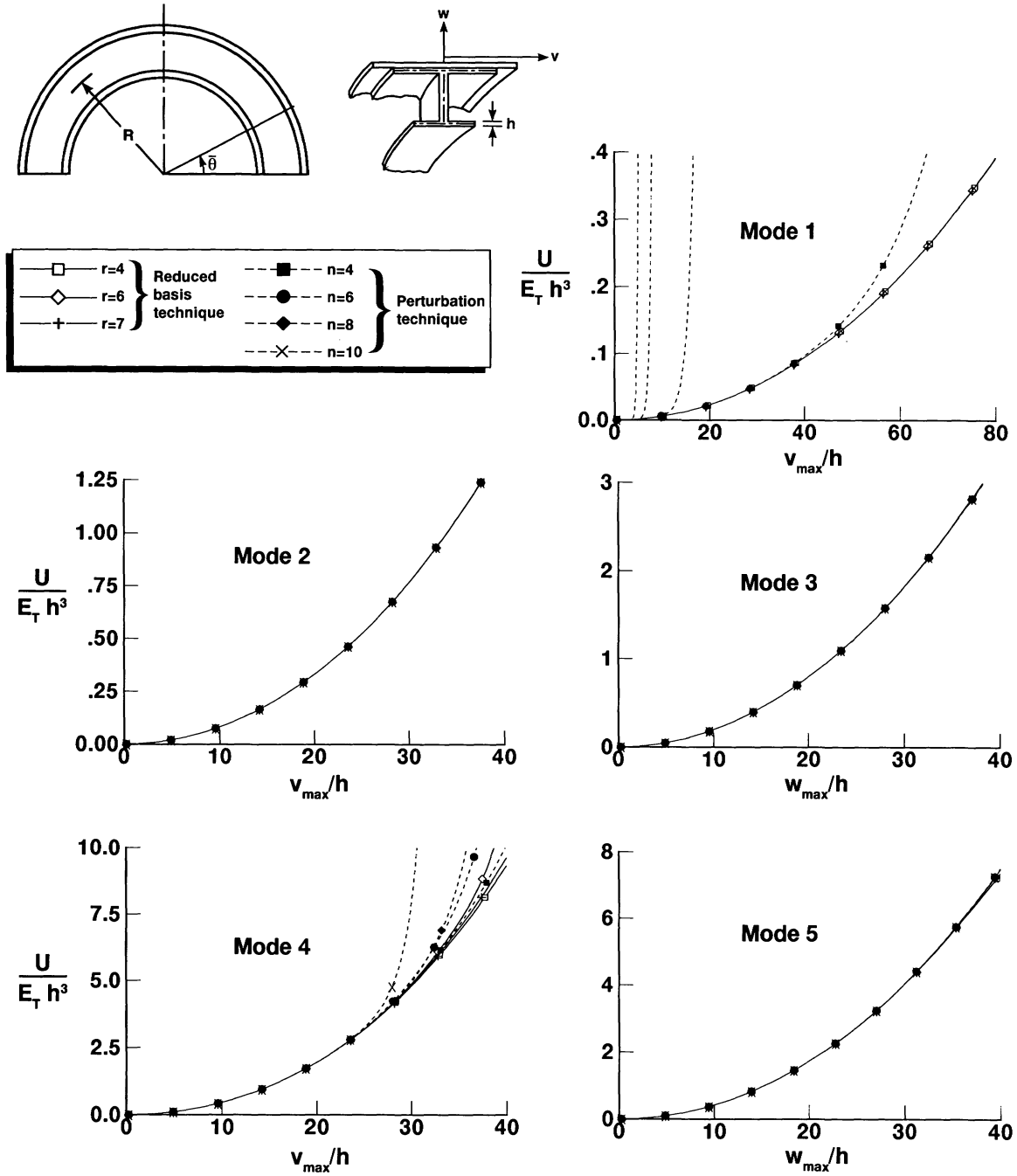


**FIGURE 3** Convergence of total complementary strain energy obtained by reduced basis and perturbation techniques. Thin-walled composite frame with I cross section (see Fig. 1).

The frames were discretized by using mixed finite element models with bicubic interpolation functions for each of the generalized displacements and stress resultants. The characteristics of the finite element model are given in Noor and Andersen (1982). An 18 × 8 finite element grid was used for modeling the whole I-section frame. In this grid, two elements were used to model each of the web, top flange, and bottom flange sections. The part of the skin adjacent to the top flange section was treated as part of the flange. One element was needed to model each of the two parts of the skin section that extended beyond the top flange (see Noor et al., 1991). The

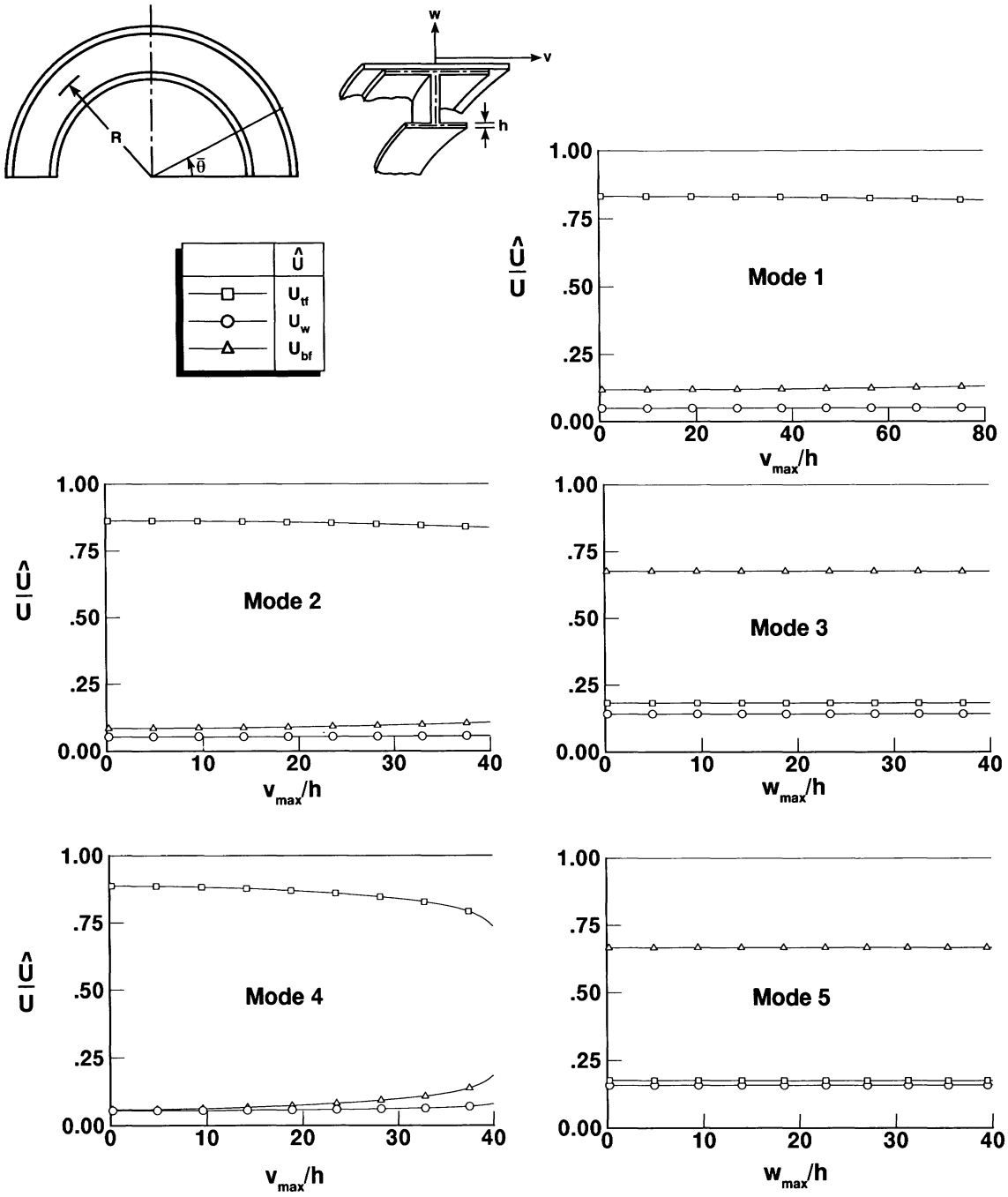


**FIGURE 4** Variation of energy components in different vibration modes, obtained by reduced basis technique, with amplitude. Thin-walled composite frame with I cross section (see Fig. 1). Subscripts tf, w, and bf refer to top flange, web, and bottom flange, respectively.

middle surfaces of the bottom flange and the web were taken to be their reference surfaces. The middle surface of the combined top flange and skin was taken to be the reference surface.

An 18 × 7 grid was used for modeling the whole J-section frame. The distribution of the elements was similar to that for the I-section frame. Only one element was used to model the bottom flange section.

The perturbation parameter $\varepsilon$ was selected to

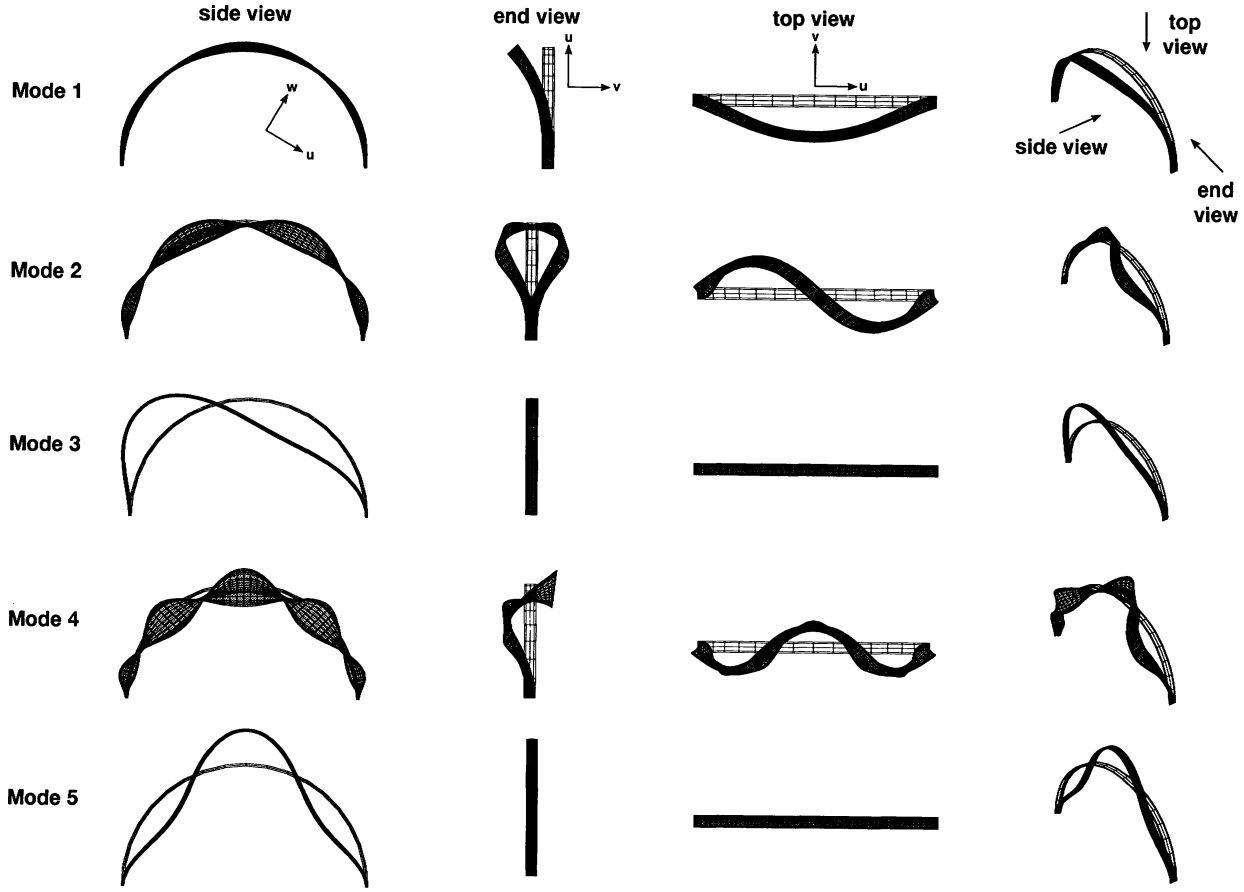


**FIGURE 5** Mode shapes associated with lowest five nonlinear frequencies. Thin-walled composite frame with I cross section (see Fig. 1).

be the coefficient of the linear vibration mode [$\psi_1$ in Eq. (10)], and the Linstedt–Poincaré method was used to generate perturbation vectors and their derivatives, up to order 10 of $\varepsilon$ [$n = 10$, where $n$ is the highest-order term in the perturbation series of $\Omega$, $\{H\}$, and $\{X\}$ in Eqs. (5), (6), (8), and (9)].

The perturbation vectors were used as coordinate vectors, and a direct variational technique was applied to determine the nonlinear frequency and the amplitudes of the coordinate vectors [$\psi_1$ in Eq. (10)]. The perturbation vectors and their derivatives, Eq. (11), were then used in conjunction with a direct variational technique to determine the parameters $\bar{\psi}_i$ and the sensitivity coefficients $\partial\omega^2/\partial\lambda$ [Eqs. (11) and (B.1), Appendix B] corresponding to different values of $\varepsilon$. The sensitivity coefficients were validated by comparing them with the finite difference results. Very close agreement was observed between both. Typical results are shown in Figs. 2–6 for the I-section frame, and in Figs. 7–11 for the J-section frame.

## I-Section Frame

The accuracy and convergence of the nonlinear vibration frequencies and total complementary strain energies $U$, associated with the first five modes, obtained by the reduced basis and perturbation techniques, are shown in Figs. 2 and 3. The rapid convergence of the solutions obtained by the reduced basis technique is demonstrated for amplitudes up to 80 times the flange thickness for the first mode (and up to 40 times the flange thickness for the other four modes). The perturbation solutions diverge for $v/h > 10$ for the first mode, and for $v/h > 25$ for the fourth mode. Note that a stiffening effect is observed for modes 1, 2, and 4, and a softening effect for modes 3 and 5. As expected, the total complementary strain energy increases for higher modes.

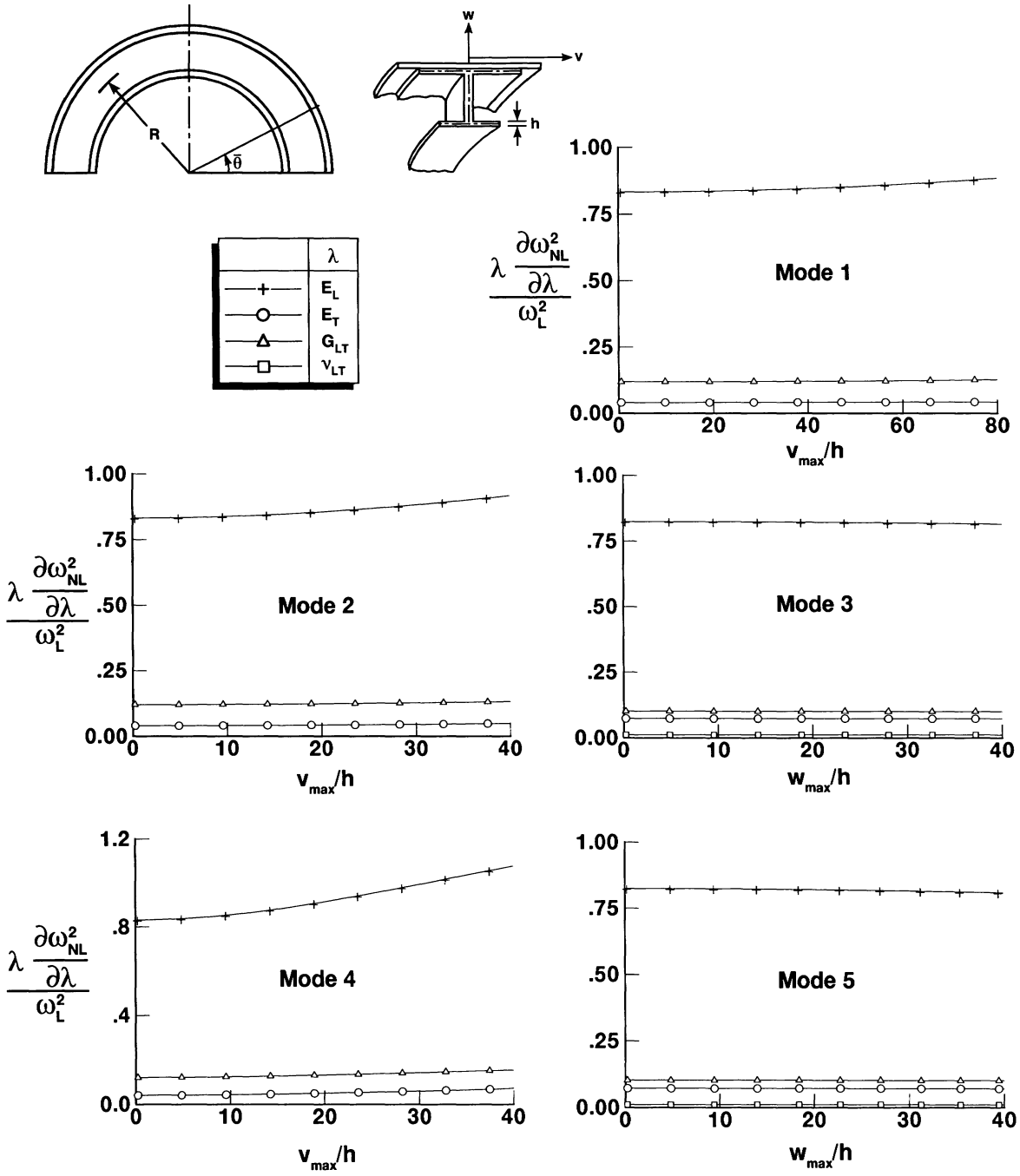


**FIGURE 6** Variation of the sensitivity coefficients, obtained by reduced basis technique with amplitude. Thin-walled composite frame with I cross section (see Fig. 1).

The total complementary strain energy associated with each mode is decomposed into three components $U_{tf}$, $U_w$, and $U_{bf}$; these components represent the contributions of the top flange (including the skin), web, and bottom flange. In Fig. 4, the variation of the ratios $U_{tf}/U$, $U_w/U$, and $U_{bf}/U$ is shown for each of the modes, with the amplitude. For the first, second, and fourth modes, the contribution of the top flange to the total complementary energy is dominant, and for third and fifth modes, the contribution of the bottom flange is dominant. The mode shapes associ-

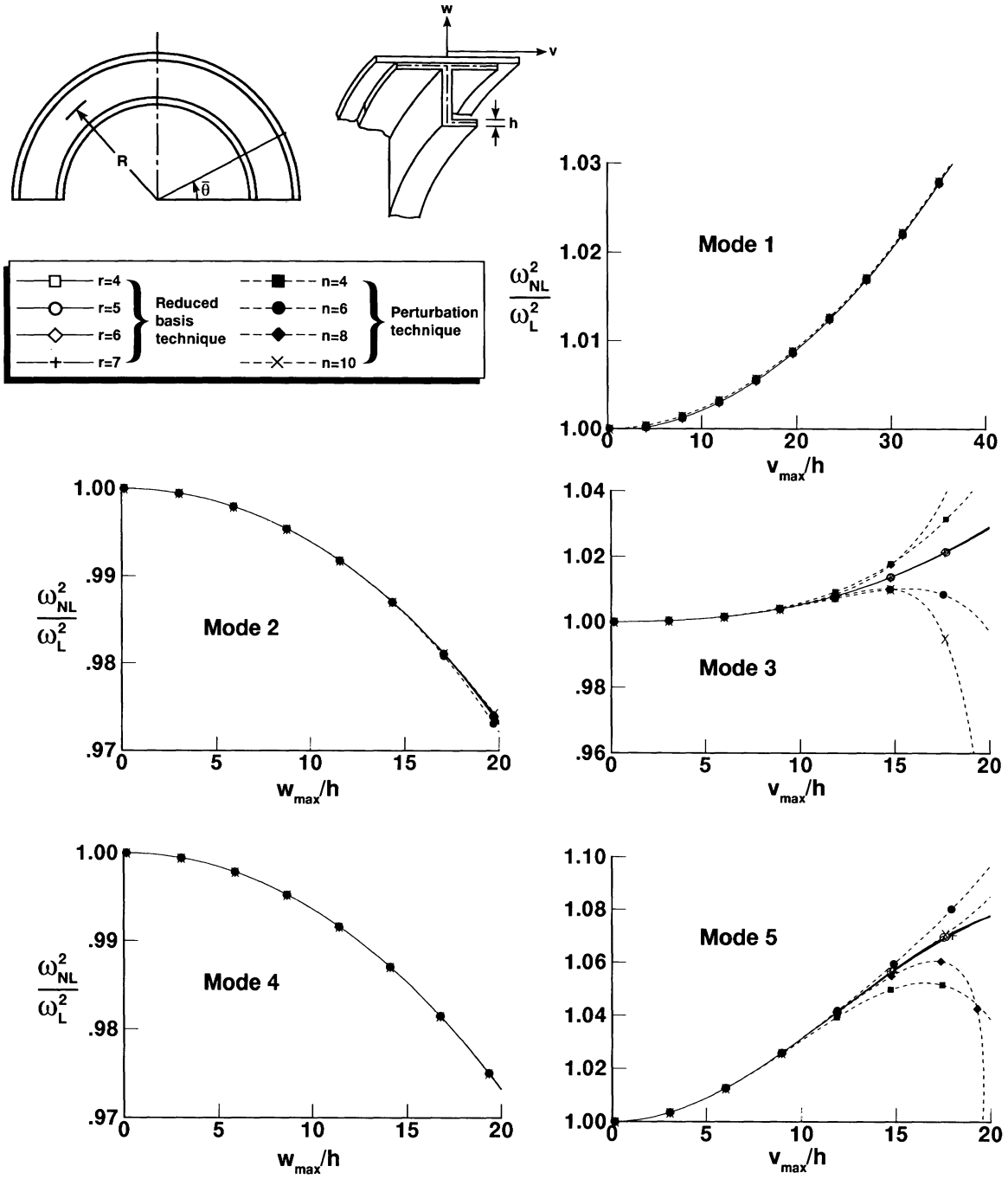


**FIGURE 7** Convergence of nonlinear frequencies obtained by reduced basis and perturbation techniques. Thin-walled composite frame with J cross section (see Fig. 1).

ated with the lowest five nonlinear frequencies are shown in Fig. 5.

Variations of the normalized sensitivity coefficients of the vibration frequencies with the amplitude are shown in Fig. 6. Each sensitivity coefficient is normalized by multiplying by $\lambda$ and dividing by the square of the linear frequency $\omega_L^2$, where $\lambda$ refers to each of the material parameters $E_L$, $E_T$, $G_{LT}$, and $\upsilon_{LT}$. As can be seen from Fig. 6, the nonlinear frequencies are very sensitive to variations in $E_L$, somewhat sensitive to variations in $G_{LT}$ and $E_T$, and insensitive to vari-

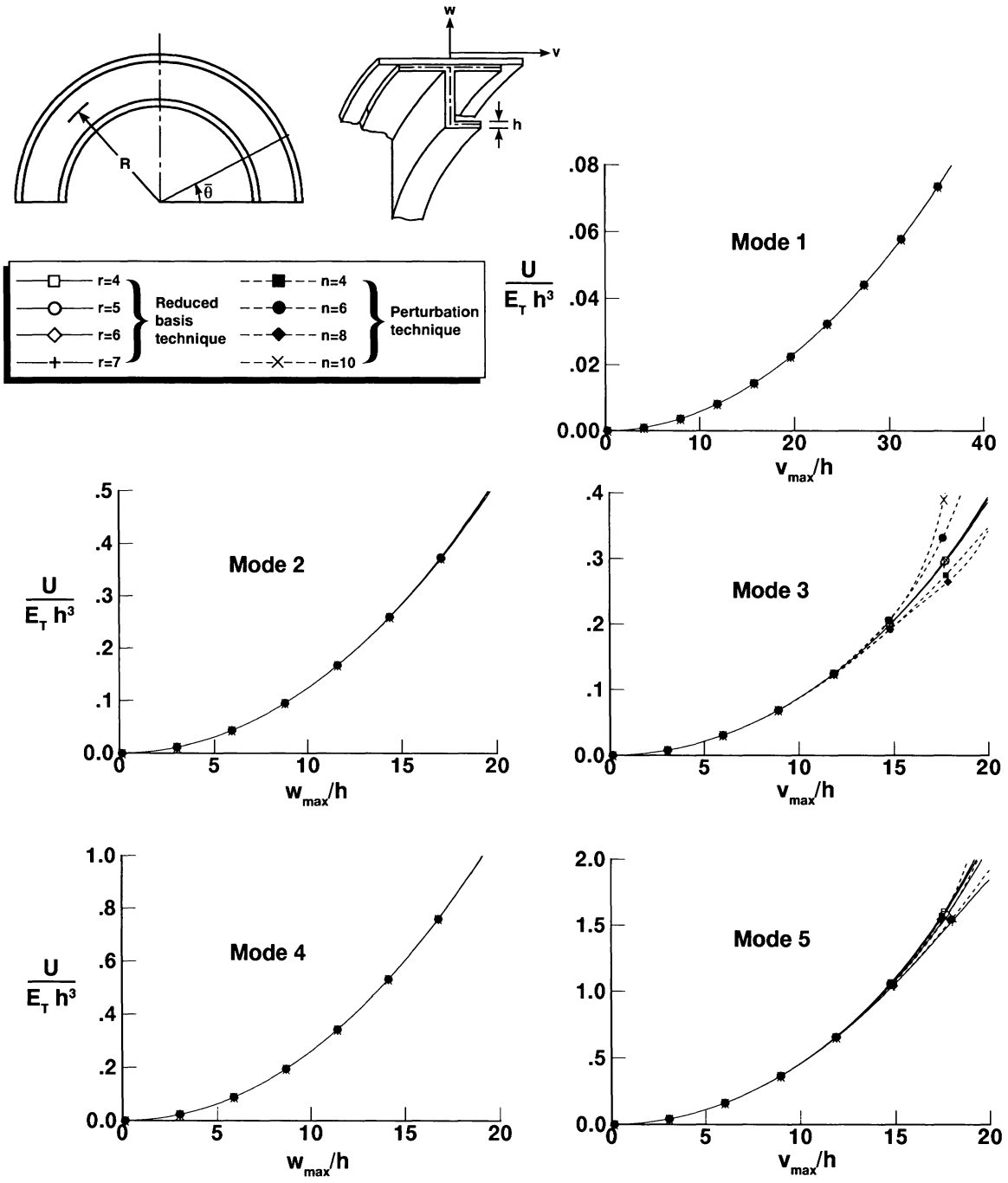


**FIGURE 8** Convergence of total complementary strain energy obtained by reduced basis and perturbation techniques. Thin-walled composite frame with J cross section (see Fig. 1).

ations in $v_{LT}$. For modes 1, 2, and 4, the sensitivity with respect to $E_L$ increases with the increase in amplitude.

## J-Section Frame

The accuracy and convergence of the nonlinear vibration frequency and the total complementary strain energies $U$, associated with the first five modes, obtained by the reduced basis and perturbation techniques, are shown in Figs. 7 and 8. Except for modes 3 and 5, the convergence of the perturbation solutions is as good as that of the reduced basis technique for the range of amplitudes considered (up to 40 times the thickness for the first mode and up to 20 times the thickness

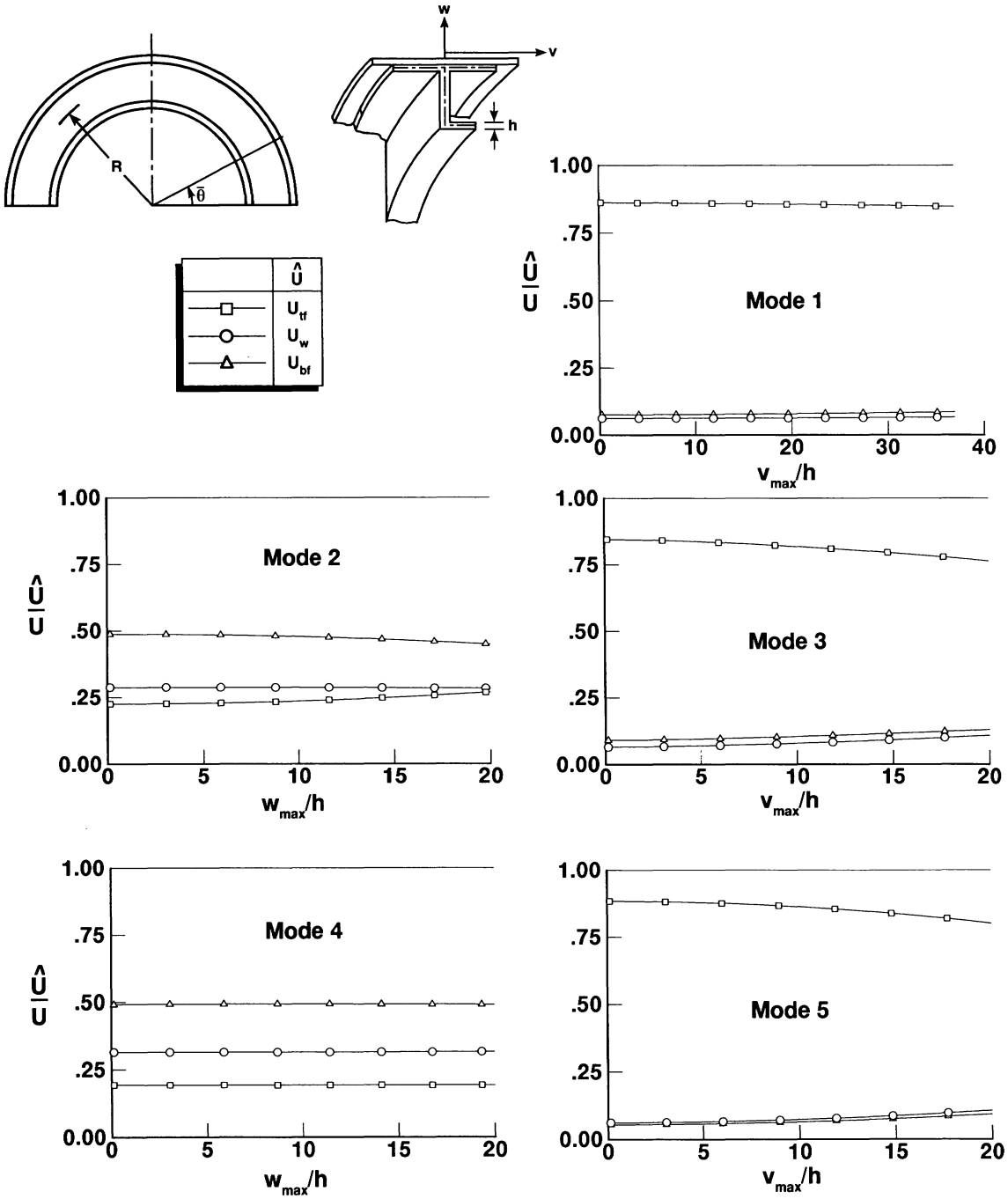


**FIGURE 9** Variation of energy components in different vibration modes, obtained by reduced basis technique, with amplitude. Thin-walled composite frame with J cross section (see Fig. 1). Subscripts tf, w, and bf refer to to flange, web, and bottom flange, respectively.

for the other four modes). As can be seen from Fig. 7, a stiffening effect is exhibited in modes 1, 3, and 5, and a softening effect in modes 2 and 4.

The variations of the ratios $U_{tf}/U$, $U_w/U$, and $U_{bf}/U$, with the amplitude, is shown in Fig. 9 for each of the five modes. The contribution of the top flange to the total complementary strain energy is dominant for modes 1, 3, and 5. In contrast, for modes 2 and 4 the contribution of the top flange to the total complementary strain energy is less than that of the bottom flange and web. The mode shapes associated with the low-

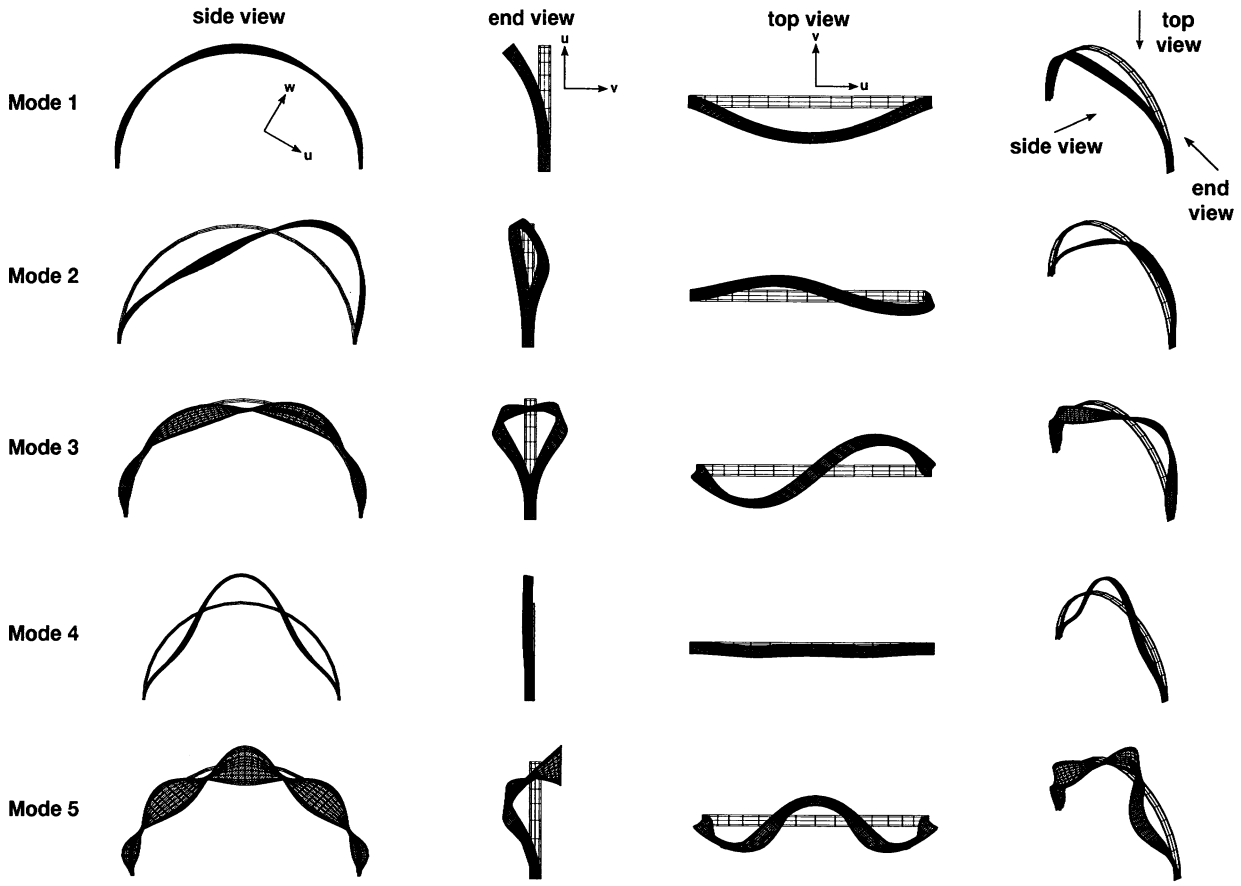


**FIGURE 10** Mode shapes associated with lowest five nonlinear frequencies. Thin-walled composite frame with J cross section (see Fig. 1).

est five nonlinear frequencies are shown in Fig. 10. Variations of the normalized sensitivity coefficients of the vibration frequency with the amplitudes are shown in Fig. 11. As for the I cross section, the nonlinear frequency is very sensitive to variations in $E_L$, somewhat sensitive to variations in $G_{LT}$ and $E_T$, and insensitive to variations in $\upsilon_{LT}$. For modes 1, 3, and 5 the sensitivity coefficient with respect to $E_L$ increases with the increase in amplitude.

## CONCLUSIONS

A reduced basis technique and a computational procedure are presented for generating the nonlinear vibrational response, and evaluating the first-order sensitivity coefficients of thin-walled composite frames (derivatives of the nonlinear frequency with respect to material and geometric parameters of the plate). The analytical formulation is based on the moderate rotation, geometrically nonlinear Sanders–Budiansky type shell theory with the effects of transverse shear deformation, laminated anisotropic material response, rotatory inertia, and large displacements included. The frames are discretized by using mixed finite element models with the fundamental unknowns consisting of both generalized nodal displacements and stress resultant parameters of the frame.

The computational procedure can be conveniently divided into three distinct steps. The first step involves the generation of various-order perturbation vectors and their derivatives with respect to the material and lamination parameters of the frame, using the Lindstedt–Poincaré perturbation technique. The second step consists of using the perturbation vectors as basis vectors, computing the amplitudes of these vectors and the nonlinear frequency of vibration via a direct variational approach. The third step consists of using the perturbation vectors, and their derivatives, as basis vectors and computing the sensitivity coefficients of the nonlinear fre-

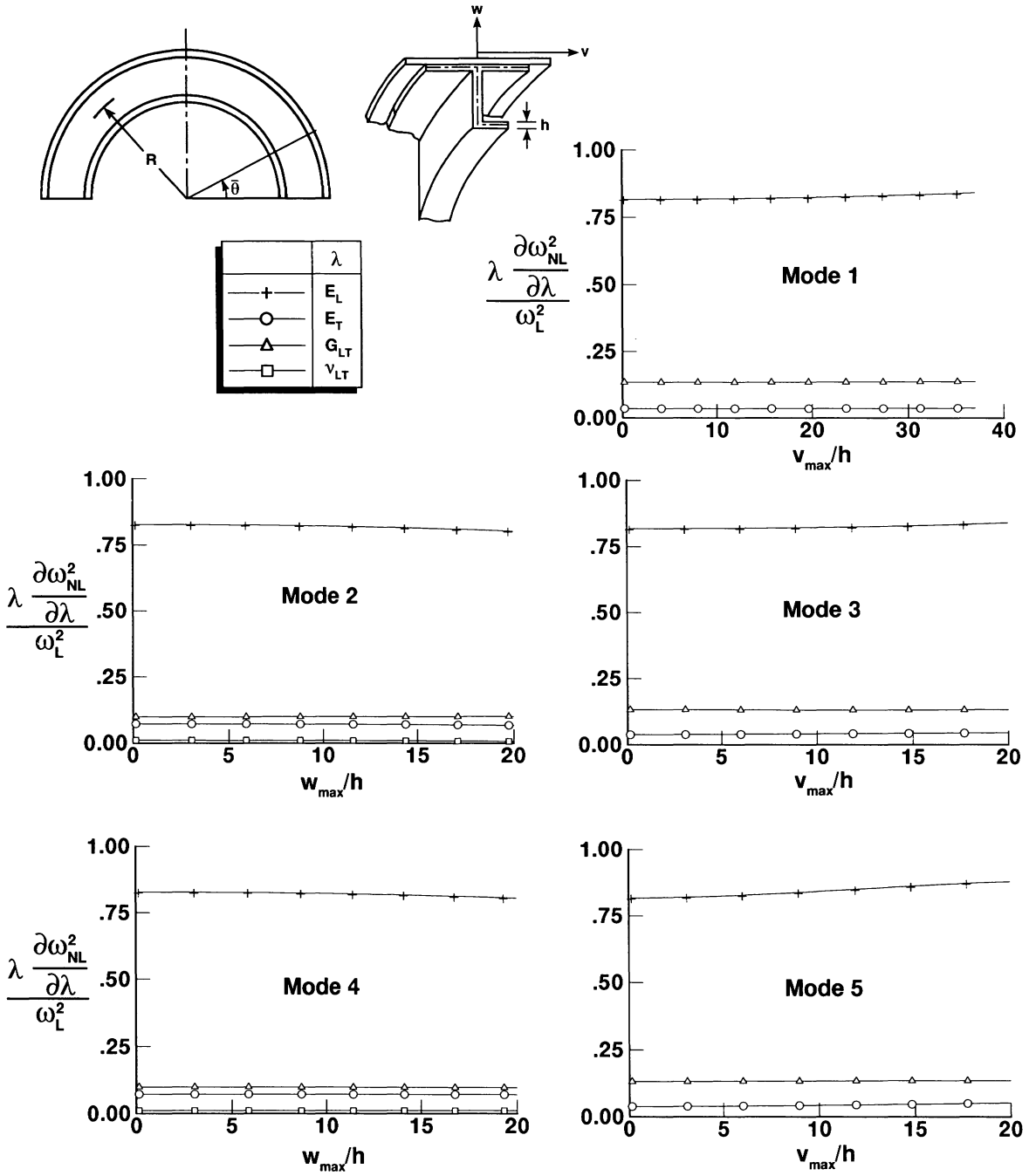


**FIGURE 11** Variation of the sensitivity coefficients, obtained by reduced basis technique with amplitude. Thin-walled composite frame with J cross section (see Fig. 1).

quency via a second application of the direct variational procedure. The effectiveness of the reduced basis technique is demonstrated by means of numerical examples of semicircular thin-walled frames with I and J sections.

On the basis of the present study, the following two observations can be made.

1. The reduced basis technique can be thought of as either a generalized perturbation technique in which the response vectors contain free parameters rather than fixed coefficients and the perturbation parameter need not be small; or an extension of the direct variational technique with the

coordinate vectors generated by using a perturbation technique rather than chosen *a priori*.

2. The successive application of the perturbation technique and the direct variational procedure, which forms the basis of the foregoing reduced basis technique, results in enhancing the effectiveness of the direct variational technique by removing (or reducing) the arbitrariness in the selection of the coordinate vectors, and extending the range of applicability of the regular perturbation technique by removing the restriction of a small perturbation parameter.

This research was partially supported by NASA Cooperative Agreement NCCW-0011 and by NASA Grant NAG-1-1197. The authors acknowledge useful discussions with Samuel L. Venneri, Robert J. Hayduk, and Huey D. Carden of NASA.

## REFERENCES

Bert, C. W., 1982, "Research on Dynamics of Composite and Sandwich Plates, 1979–1981," *The Shock and Vibration Digest,* Vol. 14, No. 10 pp. 17–34.

Chia, C. Y., 1980, *Nonlinear Analysis of Plates,* McGraw–Hill, New York.

Chia, C. Y., 1988, "Geometrically Nonlinear Behavior of Composite Plates: A Review," *Applied Mechanics Reviews,* Vol. 41, pp. 439–451.

Kapania, R. K., and Raciti, S., 1989, "Recent Advances in Analysis of Laminated Beams and Plates, Part II: Vibrations and Wave Propagation," *AIAA Journal,* Vol. 27, pp. 935–946.

Kapania, R. K., and Yang, T. Y., 1987, "Buckling, Postbuckling and Nonlinear Vibrations of Imperfect Plates," *AIAA Journal,* Vol. 25, pp. 1338–1346.

Nayfeh, A. H., and Mook, D. T., 1979, *Nonlinear Oscillations,* John Wiley, New York.

Noor, A. K., and Andersen, C. M., 1982, "Mixed Models and Reduced/Selective Integration Displacement Models for Nonlinear Shell Analysis," *International Journal for Numerical Methods in Engineering,* Vol. 18, pp. 1429–1454.

Noor, A. K., Andersen, C. M., and Peters, J. M., 1993, "Reduced Basis Technique for Nonlinear Vibration Analysis of Composite Panels," *Computer Methods in Applied Mechanics and Engineering,* Vol. 103, pp. 175–186.

Noor, A. K., Carden, H. D., and Peters, J. M., 1991, "Free Vibrations of Thin-Walled Semicircular Graphite-Epoxy Composite Frames," *Finite Elements in Analysis and Design,* Vol. 9, pp. 33–63.

Noor, A. K., Hadian, M. J., and Andersen, C. M., 1993, "Hybrid Analytical Technique for Evaluating the Sensitivity of the Nonlinear Vibrational Response of Beams," *Computers and Structures,* Vol. 49, pp. 569–578.

Sathyamoorthy, M., 1982a, "Nonlinear Analysis of Beams, Part I: A Survey of Recent Advances," *The Shock and Vibration Digest,* Vol. 14, No. 8 pp. 19–35.

Sathyamoorthy, M., 1982b, "Nonlinear Analysis of Beams, Part II: Finite Element Methods," *The Shock and Vibration Digest,* Vol. 14, No. 9 pp. 7–18.

Sathyamoorthy, M., 1987, "Nonlinear Vibration Analysis of Plates: A Review and Survey of Recent Developments," *Applied Mechanics Reviews,* Vol. 40, pp. 1553–1561.

## APPENDIX A: FORM OF NONLINEAR EQUATIONS IN $\psi_i$ AND $\omega$

The nonlinear algebraic equations in the amplitudes of the coordinate functions $\psi_i$, and the frequency $\omega$, can be written in the following compact form:

$$K_{ij}\psi_j + F_{ijk}\psi_j\psi_k + G_{ijks}\psi_j\psi_k\psi_s - \omega^2 M_{ij}\psi_j = 0 \tag{A.1}$$

where the range of $i$, $j$, $k$, and $s$ is $1$–$r$, and a repeated index in the same term denotes summation over its full range. The arrays $K_{ij}$, $F_{ijk}$, $G_{ijks}$, and $M_{ij}$ are obtained by using Eqs. (10), (3), (4), and (1), applying the method of harmonic balance, and performing the temporal integration.

## APPENDIX B: FORM OF LINEAR EQUATIONS IN $\bar{\Psi}_i$ and $\partial\omega^2/\partial\lambda$

The linear algebraic equations in the amplitudes of the coordinate functions $\bar{\psi}_i$, used in approximating the derivatives of the displacement parameters, and the sensitivity coefficients $\partial\omega^2/\partial\lambda$, can be written in the following compact form:

$$\begin{aligned}[(K_{ij} + 2F_{ijk}\psi_k + 3G_{ijks}\psi_k\psi_s) &- \omega^2 M_{ij}]\bar{\psi}_j - M_{ij}\psi_j \frac{\partial\omega^2}{\partial\lambda} \\ &= -\left[\left(\frac{\partial K_{ij}}{\partial\lambda} + \frac{\partial F_{ijk}}{\partial\lambda}\psi_k + \frac{\partial G_{ijks}}{\partial\lambda}\psi_k\psi_s\right)\right. \\ &\quad \left. - \omega^2 \frac{\partial M_{ij}}{\partial\lambda}\right]\psi_j .\end{aligned} \tag{B.1}$$

Note that the $\psi$'s appearing on the left-hand side of Eq. (B.1) are obtained from Eq. (A.1). The $K$, $F$, $G$, and $M$ arrays appearing on the left-hand side of Eq. (B.1) are in terms of $\{H\}^{(i,m)}$ and $\{X\}^{(i,m)}$. The corresponding arrays on the right-hand side are in terms of the corresponding $(\partial/\partial\lambda)\{H\}^{(i,m)}$ and $(\partial/\partial\lambda)[X]^{(i,m)}$.